Sensors & Actuators: B. Chemical 401 (2024) 135027

Contents lists available at ScienceDirect

Sensors and Actuators: B. Chemical

journal homepage: www.elsevier.com/locate/snb

Ion-selective organic electrochemical transistors for the determination of potassium in clinical samples

Marc Clua Estivill, Adil Ait Yazza, Pascal Blondeau, Francisco J. Andrade *

Departament de Química Analítica I Química Orgànica Universitat Rovira i Virgili (URV), C/Marcel·li Domingo 1, Tarragona 43007, Spain

ARTICLE INFO

Keywords:
Ion detection
Organic electrochemical transistors
Paper-based sensors
Potassium
PEDOT:PSS

ABSTRACT

The development and optimization of a paper-based ion-selective organic electrochemical transistor (IS-OECT) with an outstanding analytical performance is presented. The combination of thick-film transistor technology with a suitable optimization of the ion-selective membrane composition and thickness allows reaching sensitivities of up to 2.50 mA/decade, which is more than one order of magnitude higher than other similar devices reported up to date. The system shows good selectivity, allowing the detection of low concentrations of potassium in high saline concentrations, and a linear range from 0.1 mM to 100 mM, which covers the relevant clinical range of K^+ in blood. A calibration curve for K^+ in artificial serum between 1 and 10 mM shows changes in concentrations down to 0.05 mM can be discriminated. Furthermore, the device can be made with a simple manufacturing process, such as drop casting, on low-cost substrate materials and can be operated with a gate voltage of 0 V. This IS-OCET offers promising avenues for developing ion-sensing platforms for the point of need.

1. Introduction

The determination of ions in solution plays an central role in multiple areas, such as clinical analysis, environmental monitoring, and industrial processes control, among many others [1,2]. In clinical samples, the determination of major ionic components -such as Na^+ or K^+- represents a unique analytical challenge. Discriminating small variations of analyte concentrations in samples with a high ionic background requires techniques with high sensitivity and selectivity [3]. For K^+ in blood, for example, sub-mM differences must be accurately assessed for concentrations ranging from 3 to 7 mM, in a matrix that is typically 135 mM in Na^+ [4]. Atomic spectroscopy techniques show high sensitivity, but narrow linear ranges at low concentrations. Thus, the high degree of dilution required add potential sources of error. Ion-selective electrodes (ISEs), on the other hand, show a wide linear range and high selectivity, thus offering unique advantages for the detection of ions in whole, undiluted clinical samples [5]. As a downside, due the logarithmic response and the limited Nernstian sensitivity, highly relevant clinical variations produce very small changes of the analytical signal. As a result, these systems often need to work under highly controlled conditions. This problem needs to be addressed when developing devices for the point of need.

Improvements introduced by Ion-selective field-effect transistors (ISFETs) have not managed to successfully overcome many of the limitations of ISEs [6,7]. Alternatively, Bobacka et al. have recently shown that the discharge current produced by short-circuiting the ISE and the reference electrode can be used to improve the performance of ISEs [8]. This coulometric transduction, recently refined by Bakker *et al.* through a precise potential control mechanism, provides a very attractive path to enhance the sensitivity, showing promise for the development of clinical tools [9]. Alternative strategies, such as connecting electrochemical cells in series have been also proposed [10]. However, they are more complex to implement in real scenarios.

During the last two decades, organic electrochemical transistors (OECT) have gained popularity to build chemical and biochemical sensors due to their unique power amplification characteristics [11,12]. The concept introduced by Wrighton et al. [13] gained momentum with the widespread availability of solution-processable conducting polymer films. The working mechanisms of these devices have been extensively reviewed in the literature [11]. In essence, in OECTs an organic semiconducting film (the channel) connects two electrodes: the source (S) and the drain (D). The channel is often made with the conducting polymer poly(3,4-ethylenedioxythiophene) doped with polystyrene sulphonate (PEDOT:PSS). This ensemble (Source-channel-Drain) is immersed in an aqueous solution. With the S grounded, a constant negative voltage (V_d) is applied to D, generating a current in the channel

* Corresponding author.
E-mail address: franciscojavier.andrade@urv.cat (F.J. Andrade).

https://doi.org/10.1016/j.snb.2023.135027
Received 25 July 2023; Received in revised form 13 November 2023; Accepted 18 November 2023
Available online 22 November 2023

(I_d) that will be used as the analytical signal. A third electrode -the gate (G)- immersed into the same solution (Fig. 1A) is biased with a positive voltage (V_g) forcing the transport of cations towards the channel. Since in OECTs the channel is in direct contact with the solution, cations can migrate into the channel producing a drop in the electronic conductivity of the PEDOT:PSS, that results in a drop in I_d. Since this process is controlled by V_g, changes in V_g are reflected as changes in I_d. This is the foundation of the transduction mechanism of the OECTs [14].

The functionalization of G to generate a concentration-dependent V_g is the most common approach to build OECTs sensors. This has been used for monitoring humidity [15], pH [16], and the concentration of hydrogen peroxide [17], glucose [18] ethanol [19], a large number of biomolecules [20,21], etc. Many of these systems have been used to build low-cost disposable devices and wearable sensors [22–24]. Our group has shown that the OECT sensor performance can be boosted by using thick-film PEDOT:PSS channels [17].

While OECTs are often associated to potentiometric sensors with a unique transduction mechanism [25], using ISEs as gate electrodes shows poor performance [26]. To achieve an effective gating most of the V_g must drop in the vicinity of the channel. For this reason, gates with a negligible gate capacitance, e.g., Ag/AgCl, are often used. Since ISEs have a large capacitance, when used as a gate the applied V_g drops in the vicinity of the electrode. This leads to a poor OECT performance.

Since OECT sensors can be also made by functionalizing the surface of the channel [21,27], coating channel with an ion-selective membrane (ISM) has been proposed [28]. The performance obtained for the detection of sodium was modest (sensitivity of 50 μA/dec), but was better than the ISE-gated devices. A similar approach has been used to develop a wearable patch to monitor ions in sweat [22]. More recently, the use of a PSS layer underneath the ion-selective membrane has allowed the improvement of the sensitivity for the determination of potassium (224 μA/dec) and sodium (98 μA/dec) [29]. Interestingly, despite of the significantly different transduction mechanisms between ISEs and ion-selective OECT (IS-OECT), the same type of membranes have been employed in both cases.

This work introduces an approach to build IS-OECT with an outstanding response and simple manufacturing and operation. Thick-film channel technology [17] is used to achieve high levels of trans-conductance, while optimization of the membrane chemical and morphological characteristics leads to an enhanced performance. These devices show a sensitivity that can reach up to 2.5 mA/decade at $V_g = 0$ V. This simplifies the operation of the device and may allow in the future the integration of the gate electrode in the source. Also, instead of the complex and tedious processes a simple drop casting approach is used to build paper-based IS-OECT [23]. The determination of K^+ in artificial serum in the single mM range illustrates the potential of this approach to become a useful tool for point of care applications.

2. Experimental

2.1. Materials and methods

All chemicals used were analytical grade from Sigma-Aldrich (SI). Potassium tetrakis(4-chlorophenyl) borate was used as ion-exchanger (IE). Valinomycin as K^+ ionophore. The polymeric structure of the membrane is given by the polymer polyvinyl chloride (PVC) and the plasticizer 2-Nitrophenyl octyl ether (NPOE). We call the combination of these two components Polymeric material (PM).

Details of the preparation of the ion-selective membrane (ISM) can be found elsewhere [30]. Membrane components were dissolved in THF, sonicated for 10 min and stored at 8 °C. The composition of the different membranes used is provided in Table 1.

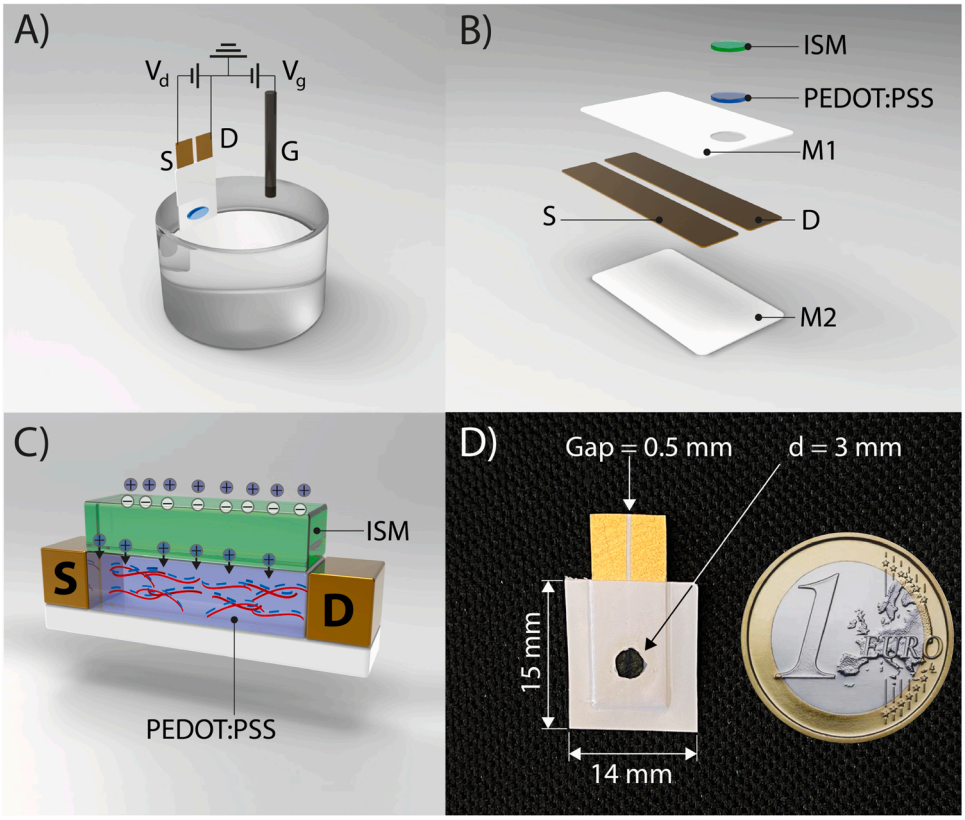

Fig. 1. Scheme of IS-OECT setup and fabrication. A) Illustration of the typical components of an OECT: source (S), drain (D) and gate (G); V_d = source-drain voltage; V_g = gate voltage. B) Schematics of the construction of a paper-based channel with the S and D electrodes sputtered on paper, shielded by plastic masks (M1 and M2). The PEDOT:PSS channel (cast on the window mask) and ion-selective membrane (ISM) (cast onto the conducting polymer). C) Illustration of the ISM cast onto the PEDOT:PSS channel. D) Picture and dimensions of a typical paper-based channel for the OECT.

Table 1
Composition of ion-selective membrane cocktails used in this work with PM for polymeric matrix.

Membrane	PM (wt%)		Ion-Exchanger (wt%)	Ionophore (wt%)	THF
	PVC	NPOE			
Conventional	32.8	64.7	0.5	2	1 mL/ 100 mg
PM 50 %	16.4	32.3	0.5	2	1 mL/ 51.2 mg
PM 33 %	10.9	21.6	0.5	2	1 mL/ 35 mg
PM 25 %	8.2	16.2	0.5	2	1 mL/ 26.9 mg
Blank	10.9	21.6	0.5	—	1 mL/ 33 mg
PM	10.9	21.6	—	—	1 mL/ 32.5 mg

2.1.1. Instrumental setup

A diagram of device setup is shown in Fig. 1A. Two power supplies (TENMA, Element14, Newark, New Jersey, US) with a common ground were used for the application of V_g and V_d. The S electrode was grounded, and a negative voltage was applied to D. Positive voltage was applied to G, which was made with a 2 × 4 mm Ag/AgCl flat tip probe (Warner INSTRUMENTS, Holliston, MA, USA). A Keithley 6514 Electrometer (Keithley Instruments, Cleveland, OH, USA) was connected in series with the channel to monitor I_d.

2.1.2. OECT fabrication and operation

Details on the fabrication of a thick-film OECT can be found elsewhere [17]. Briefly, to create the conductive tracks (S and D electrodes) a 0.5 mm adhesive tape is first applied onto a paper substrate and then a 100 nm Au layer is sputtered on top. When the adhesive tape is removed two Au electrodes separated by a 0.5 mm gap (S and D) are created. Fig. 1B shows the different components and assembly of the S-D channel system. A mask made with a water-resistant adhesive paper and having a 3 mm diameter window was used to block the Au pads, leaving only a small fraction of the electrodes exposed. A 1.5 μL PEDOT:PSS solution is drop cast onto the window covering all the exposed region. After drying at room temperature, the channel is baked for 20 min at 100 °C. The channel resistance (between S and D) is 10.2 ± 0.4 Ω (N = 4), allowing high currents with low applied voltages. In this work, a V_d = –0.4 V was applied, leading to currents in the order of 25 mA for bare PEDOT:PSS channels.

The electrical characterization of the device was performed in 0.1 M KCl. For the analytical performance, $MgCl_2$ 0.1 M and artificial serum: NaCl (6.487 g/L), $NaHCO_3$ (2.436 g/L), K_2HPO_3 (0.383 g/L), $MgCl_2(6\ H_2O)$ (0.162 g/L), urea (0.150 g/L) and glucose (0.847 g/L) were used respectively. All the solutions, unless otherwise specified, were diluted in MilliQ water with resistivity 18.2 MΩ/cm (25 °C), SYNERGY® UV SYSTEMS, Merck KGaA, Darmstadt.

Germany).

2.1.3. Channel functionalization

5 μL of a membrane cocktail are drop cast on top of the dried PEDOT:PSS channel surface and the membrane is let dry. This process is repeated until a total of 15 μL of ISM cocktail have been deposited and the ISM is let dry overnight (Fig. 1C). Before using the channel is conditioned 1 h in a KCl 10^{-1} M solution and then rinsed 3 times in water for 5 min.

It has been reported that IS-OECT performance was improved by using an intermediate polyelectrolyte layer [28]. Preliminary experiments in our lab show that this thick-channel system this approach presented problems of instability due to poor membrane adhesion. Alternatively, before casting the membrane the PEDOT:PSS channel was conditioned in a KCl 10^{-1} M solution (primary ion) for 1 h. This step showed a significant improvement of the performance, suggesting that it can effectively create internal ion reservoirs, as it will be discussed below. Thus, this conditioning step was added to the preparation of all the sensors.

3. Results and discussion

A typical transfer curve of an OECT using an uncoated thick-film PEDOT:PSS channel (Fig. 2A and B) shows the reduction of I_d with the increment of V_g. This change is due to the shift in the balance of redox species of the conducting polymer. It its reduced form PEDOT is non-conductive (de-doped), while the oxidized form is highly conductive due to a large concentration of holes with high mobility (doped) [31]. The reduced PEDOT is more stable, but the electrostatic effect produced by the negatively charged sulphonate groups of PSS stabilizes the positive charges (holes) of the oxidized PEDOT, turning PEDOT:PSS into a good electronic conductor. Cations injected into the channel shield the effect of the sulphonates inducing a shift towards the reduced state that decreases the channel electronic conductivity. These variations in V_g translated into changes in I_d -the essence of the amplification mechanism of OECTs- are measured by the transconductance (g_m) [11,32]:

$$g_m = -\frac{\Delta I_d}{\Delta V_g} \quad (1)$$

Being directly linked to the sensitivity, optimizing the transconductance of an OECT is key in any analytical technique. Due to the use of thick film channels [16], g_m reaches values close to 40 mS, which is amongst the highest values achieved for this type of devices (Fig. 2C) [12]. With operating currents reaching up to several mA, the low-power input signal (gate potential) is transformed into a high-power output signal [11]. This coupled transduction-power amplification is important for signal processing. Although thick-film technology shows slower response time, the increase in sensitivity is a favorable trade-off for chemical sensors. For this reason, this type of approach has been used in all the experiments.

Although the gating of OECTs is often explained through the migration of ions from the solution, when the channel is covered by a polymeric membrane this transport is blocked. Transmembrane ion fluxes have been suggested [22], but it is unclear whether this can effectively occur in a reasonable timescale. Interestingly, it has been shown that the electrical field created by the gate can induce the movement of cations loosely trapped within the PEDOT:PSS phase. These “internal ion reservoirs” have been used to improve the response time of conventional OECTs [33]. By analogy, when the channel is coated with a polymeric membrane, gating could be ascribed to the capacitive coupling of V_g through the polymeric membrane and the existence of internal ion reservoirs (Fig. 2D). This concept is similar to the electrolyte-gated organic field transistor (EGOFET) reported by List-Kratochvil *et al.*, who used an inner electrolyte solution between the membrane and the conductive polymer [34]. In fact, the addition of an intermediate layer of a polyelectrolyte (PSS) between the ISM and the channel has been used to enhance the response of the IS-OECT [29].

In this type of mechanism, the membrane thickness and polarizability will play a key role in the sensor performance, since it will determine the effective V_g acting upon the internal ion reservoir. ISM composition and thickness have been optimized for their use in potentiometric sensors [5]. These system rely on concentration gradients at the membrane-solution interface and are designed to avoid transmembrane fluxes. Optimum ISM for ISEs have thickness in the order of 10–20 μm and impedances in the 10^5 to 10^6 Ω range. These are not necessarily optimum conditions for OECTs. In fact, preliminary experiments using a channel coated with a conventional ISM show that a maximum transconductance around 15 mS is reached at V_g slightly above 0.6 V (Fig. S1). This relatively high V_g is needed to compensate the attenuation of the field produced by the thick membrane. The major issue of this system is that selectivity is compromised, as it will be

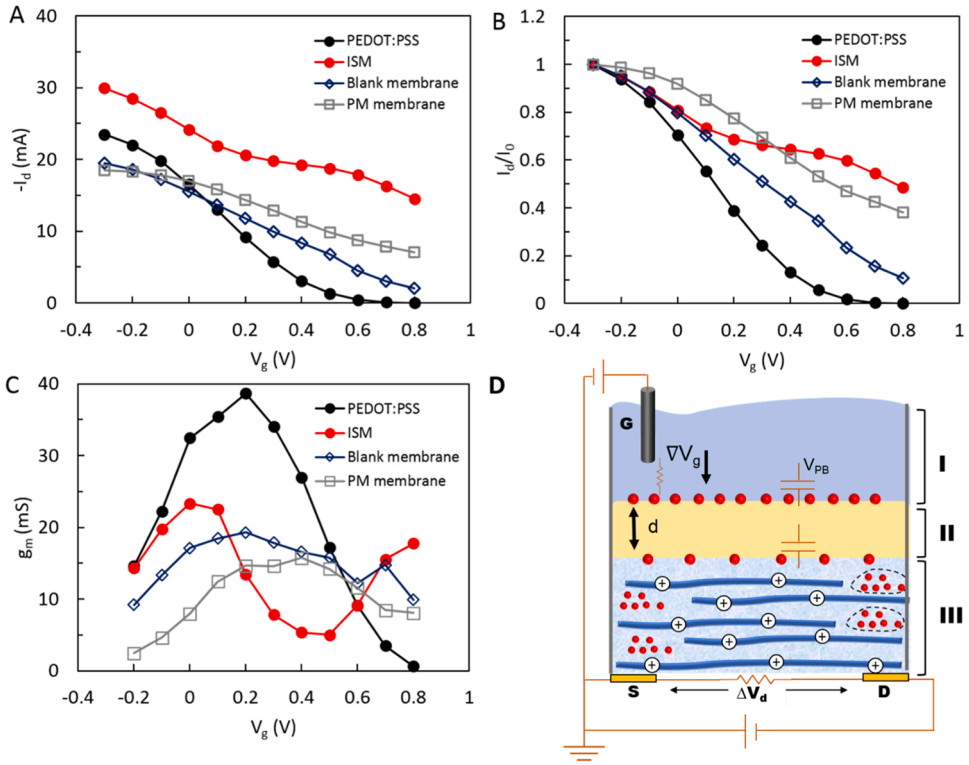

Fig. 2. : Electrical characterization of sensors made with different membranes: PEDOT:PSS (bare channel, no membrane added), ISM added (IS-OECT), Blank membrane and PM membrane. A) Transfer curve, B) Normalized curves, C) Transconductances vs V_g and D) Schematic illustration with the distinct IS-SOEC components, interfaces, and applied potentials, where I: solution, II: membrane, III: channel, d: membrane thickness, V_{PB} represents the phase boundary potential in the solution side. The electrical field induced by the gate electrode generates the capacitive coupling between the solution and the ISM (V_{PB}) due to cation recognition. The red lines represent the equivalent electrical circuit and components. All experiments were performed with the 33 % PM, in 0.1 M KCl, Ag/AgCl gate and V_d = –0.4 V.

discussed below.

The thickness of the ISM can be controlled through the amount of membrane cocktail deposited and the deposition techniques [35]. In this work, reducing the amount of membrane deposited is difficult because of the need to coat the whole channel area. Instead, different thicknesses were created by reducing the PM load in the cocktail. Membranes were prepared using 100 % PM (original ISM), 50 % PM, 33 % PM and 25 % PM of the original composition (See Table 1), while keeping the remaining components at the original level.

Reducing the PM content has a marked effect on the membrane thickness (Fig. 3A). The original, undiluted ISM has a thickness of 14.51 ± 1.62 μm (typical for an ISE). A sharp drop (3.49 ± 0.62 μm) is observed 50 % PM, and a smoother change is observed with further reduction of PM. The 33 % PM membrane (Fig. 3B) shows an average thickness of the membrane of 2.62 ± 0.59 μm (fluctuations are likely do to the manual casting). The 25 % PM (Fig. S2, Table S1) shows a similar value, suggesting a lower membrane density. These changes are reflected on the electrical characteristics. Electrochemical impedance spectra (Fig. S3) show that the electrical resistance of the original membrane -close to 80 kΩ- drops smoothly from ISM to 50 % PM, and then drops sharply (Fig. 3A). From 50 % PM to 25 % PM resistance drops more than one order of magnitude, reaching a final value close to 3 kΩ.

Thinner membranes with reduced impedance should favour the gating. The 25 % PM membrane, however, tends to produce long term fluctuations likely due to a poor mechanical stability. The 33 % PM membrane, on the other hand, provides a very good long-term stability. For this reason, the following experiments were performed using this reduced PM membrane. Noteworthy, these are unusual conditions for

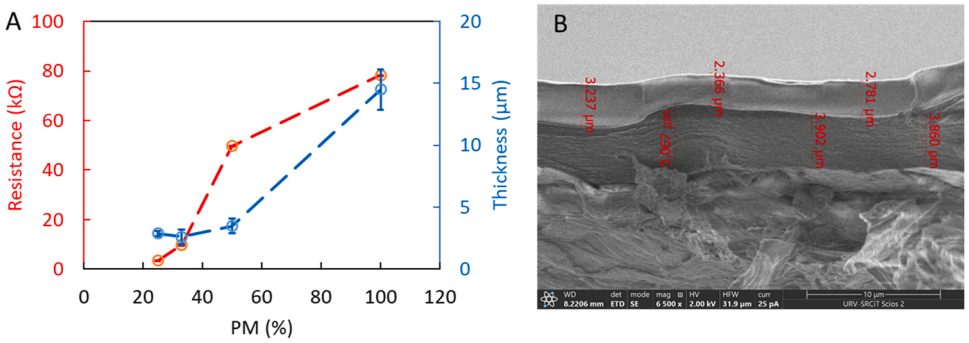

Fig. 3. : A) Influence of the dilution of the PM on the channel electrical resistance (red) and the thickness of the membrane (blue). The average membrane thickness is calculated using four cross-section zones of the channel. B) FE-SEM cross section of a IS-OECT with 33 % PM showing the PEDOT:PSS and ISM layers. Average thickness for PEDOT:PSS is 3.75 ± 0.98 and for the ISM 2.62 ± 0.59 μm.

ISEs. In fact, IS-OECTs have been typically made using thick ISM, in combination with thin channels. Demuru *et al.*, for example, reported IS-OECTs with CP films of 150 nm and ISM with thickness in the range 33–50 μm [35]. This work follows the opposite path, using thick channels (around 4 μm) and thinner ISM (around 3 μm).

In a capacitively coupled mechanism, the dielectric characteristics of the membrane and the polarizability of the interfaces should play an important role. Therefore, several experiments were conducted to gain further insights on the effect of the membrane composition on the gating characteristics. Different membrane cocktails were prepared (all with the 33 % PM) and a progressive incorporation of the ISM components (See Table 1). The PM is built just with the polymeric backbone (PVC + NPOE). The blank membrane incorporates also the ion exchanger (PM + ion-exchanger). Finally, the ISM that has all the components (Blank membrane + ionophore). Channels were coated with these membranes and the response of the different OECTs using a Ag/AgCl as a gate were compared to a bare (uncoated) channel. Tests were performed in a 0.1 M KCl solution. The results are shown in Fig. 2.

As mentioned, the bare PEDOT:PSS channel shows a maximum g_m close to 40 mS at a gate voltage ($V_{g\ max}$) of 0.2 V, which is in agreement with what has been already reported (Fig. 2C and Fig. S4) [17]. For V_g above 0.7 V the transistor is almost in the off-mode, reflecting a very efficient de-doping by ion transport into the channel. For a PM-coated channel, the reduction of g_m and the change in the gating characteristics -with I_d reduced to 40 % of the initial value at $V_g = 0.8$ V- show a reduced gating efficiency. This type of polymeric membrane, without ion-exchange capacity, dampens the electrical field. The dielectric characteristics makes gating possible, with a maximum g_m in the order of 15 mS at V_{gmax} close to 0.4 V (higher than V_{gmax} for the bare channel). In contrast, the blank membrane enhances the gating, with I_d reduced to almost 90 % of the initial value at $V_g = 0.8$ V. Clearly, the addition of an ion exchanger allows the uptake of ions and solvent, electrifying the interfaces. As a result, the g_m reaches a maximum value close to 20 mS at a $V_{g\ max} = 0.2$ V. For a channel coated with the ISM (33 % PM) g_m increases (compared to the other membranes) and reaches a maximum value of 23 mS. Interestingly, $V_{g\ max} = 0$ V. Remarkably, there is a window of V_g, between 0.3 and 0.5 V, where I_d seems unsensitive to V_g. Above 0.5 V I_d becomes once again dependent on V_g, producing a new increment on g_m. As a result, g_m shows a second increment at V_g above 0.5 V. For $V_g = 0.8$ V I_d is around 50 % of the initial value.

These results reflect the relationship between the membrane ion-exchange capacity and the gating characteristics. The gradients of electrical potential generated by the ISM are aligned with ΔV_g. Thus, the charge distribution profiles at the membrane's interfaces will respond to two different factors. First, the spontaneous extraction of ions driven by the ion-ionophore equilibrium constant and the ion exchanger (phase-boundary potential). Both, the internal (membrane/channel) and the external (membrane/solution) interfaces produce their own charge density distribution. Second, there will be a charge density induced by V_g. The gate will force cations towards the membrane, contributing to the polarization of the interface. For a thin enough membrane, the gradient of potential created spontaneously by the primary ion (K^+) seems sufficient to effectively gate the transistor. For this reason, for the IS-OECT with a thin ISM, $V_{g\ max} = 0$ V. Thicker membranes require an extra V_g to have an effective gating. Additionally, the very low trans-conductance observed for V_g 0.3–0.5 V (opposed to what is observed for the other membranes) suggests that the membrane is already loaded with the primary cation and V_g has small effect. For V_g >0.5 V, ions are forced into the membrane. This extraction should be unspecific, i.e., controlled by the hydration energies (lipophilicity) of the cation as it will be shown below.

3.1. Optimization of the analytical figures of merit

These results suggest that $V_g = 0$ V should yield a maximum sensitivity for the determination of K^+. To prove this point, calibrations curves for K^+ were performed at different V_g. All the calibrations were performed in 0.1 M $MgCl_2$ matrix to keep a constant ionic strength. The sensitivity as a function of V_g (Fig. 4A) shows a maximum value of 1.55 mA/decade at $V_g = 0$ V (see Fig. 4B for the time trace and corresponding calibration curve). For $V_g > 0$ V sensitivity drops sharply and reaches a minimum value of 0.30 mA/decade for $V_g > 0.6$ V (see Table S2). Calibrations performed at different V_d ($V_g = 0$ V) show a maximum sensitivity at –0.4 V (when maximum I_d is obtained) (Fig. 4C). V_d above –0.4 V were avoided to avoid exceeding the upper current limit of the measuring device.

Selectivity was evaluated by performing calibration curves for typical interfering cations (NH_4^+, Na^+, Li^+). All these ions show limited response, only at high concentrations and within a very narrow range (Fig. S5). Unfortunately, meaningful values of selectivity coefficients cannot be calculated because the models used with ISEs are not valid under these OECT conditions. Instead, a qualitative comparison of the selectivity was performed by measuring the total response as the difference in I_d produced by the addition of a 0.1 M solution of a given cation at different V_g. The results are measured as the subtraction of the final value of I_d (I_f) to the initial value of the current (I_0). This is an extreme comparison, that can be used to make a first estimation of the selectivity. Fig. 4D–E show that for V_g around 0 V, the relationship of these total response follows the pattern expected, i.e. the response is selective for K^+, with the major interference produced by NH_4^+. These patterns agree with a selectivity controlled by the ion-ionophore affinity.

Interestingly, at $V_g = 0.75$ V the order $NH_4^+ > K^+ > Na^+ > Li^+$ (Fig. S5E), suggests that at this high V_g the lipophilicity of the cation (Hofmeister series) instead of the ionophore affinity controls the response. This is in line with what has been previously mentioned regarding the response for K^+ at high V_g and the unspecific gate-driven membrane charging mechanism by forcing the extraction of ions into the membrane. To further prove this point, channels coated with a PM, Blank and ISM to were exposed to a 0.1 M KCl at different V_g. The results (Fig. 4F) show that while the selective behavior is observed at –0.15 V $< V_g <$ 0.15 V, at $V_g = 0.75$ V the selectivity is lost and response is higher for the blank membrane, followed by the ISM and finally the PM.

Sensor-to-sensor reproducibility was evaluated by preparing 4 different sensors and performing calibration curves for potassium. The results of the calibration with these 4 sensors can be seen in Fig. 5A. The sensitivity obtained is 1.58 ± 0.01 mA/decade of K^+, demonstrating a highly reproducible response. These data, however, have been obtained with transistors made manually and should be improved with more robust manufacturing procedures.

Evidently, the enhanced sensitivity obtained with these thick-channel thin-membrane transistors needs to be evaluated in terms of the noise levels of the systems. A major problem to make a fair comparison with other OECTs is that this type of information is not often reported in the literature. By using a battery as a power supply for V_d (as could be common in point of need devices), currents in the order of 15 mA (typically obtained for the operating V_d) can be measured with a noise level of 0.8 μA (standard deviation of baseline for a 60 s measuring interval). Therefore, currents in the single μA can be easily measured. It is also difficult to make a fair comparison with potentiometric systems, due to the different units employed. Several ways to transform currents into voltages, such as using a load resistor in line with the S-D circuit have been proposed [36], but the design and optimization of the circuit is beyond the scope of this work. In all fairness, instruments measure current by transforming it into a voltage through a shunt resistor. The Keithley 6154 used in this work provides a preamp out, which is a 2 V analog output at full scale. Considering the measuring scale used in these experiments (20 mA), the analog output provides 100 mV/mA. This means that without any additional processing, the sensitivity for the detection of K^+ is 158 mV/decade, with a noise level in the 0.1 mV range. Results from calibrations of the OECTs are compared in table S4.

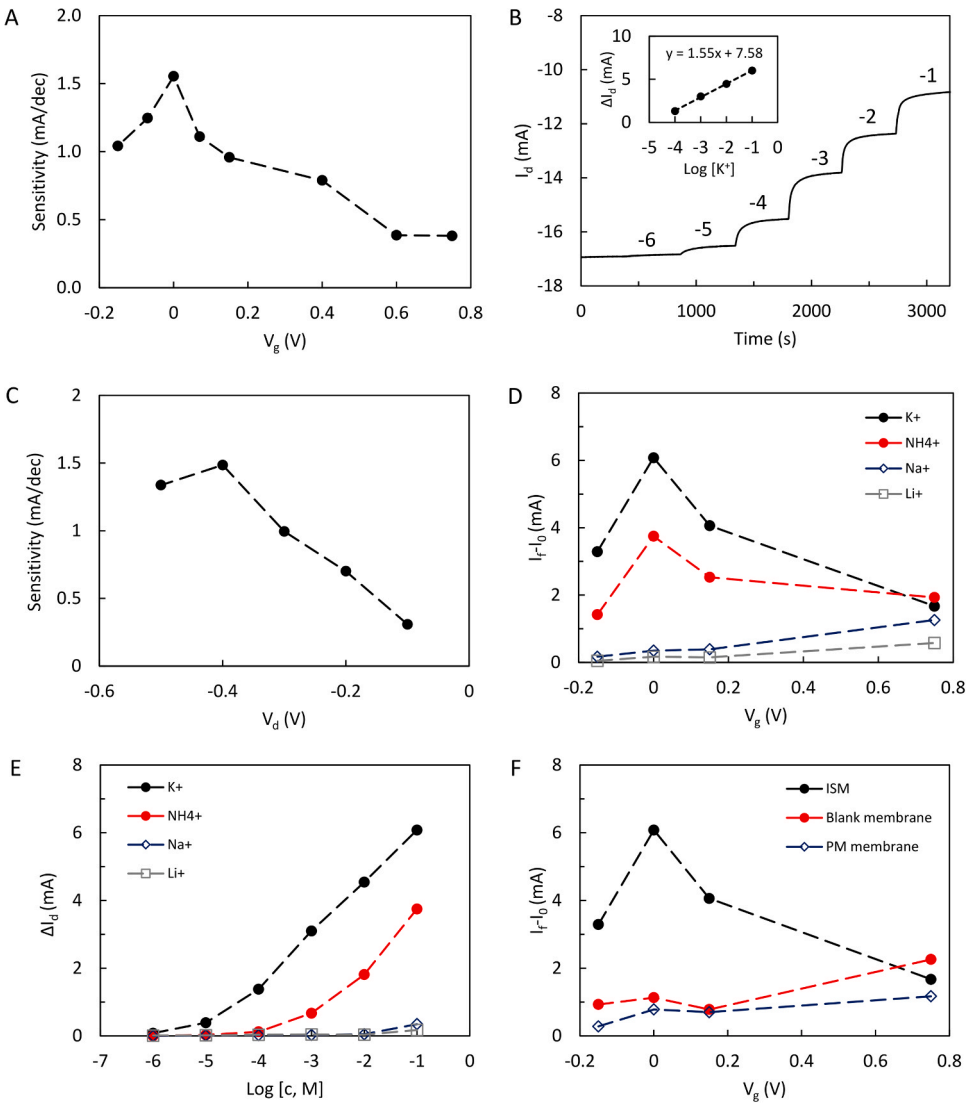

Fig. 4. : A) Sensitivity for K^+ as a function of V_g ($V_d = -0.4$ V) in the range 10^{-4} M – 10^{-1} M. B) I_d time trace upon addition of K^+ (numbers indicate the logarithm of the molar concentration of the ion) at $V_g = 0$ ($V_d = -0.4$ V). The inset shows the corresponding calibration curve. C) Sensitivity for K^+ as a function of V_d ($V_g = 0$ V). D) Total response (I_f-I_0) for the evaluation of interfering effect of common ions as a function of V_g ($V_d = -0.4$ V). E) Calibration curves for different cations ($V_g = 0$, $V_d = -0.4$ V). F) Total response for K^+ using an IS-OECT (ISM black), a blank membrane (red) and PM membrane (blue), $V_d = -0.4$ V.

3.2. Matrix composition and analytical response

To evaluate the effect of the total ion concentration on the analytical parameters and compare the results with other works presented in the literature, calibration curves for K^+ were also performed in deionized water (Fig. 5B), yielding a sensitivity of 2.58 ± 0.06 mA/decade. This value, resulting from the combination of the thick-film channel and the optimized ISM composition, is one order of magnitude higher than what has been reported up to date for similar systems [29]. Remarkably, this increase in sensitivity in distilled water does not compromise the selectivity, as seen when the response for Na^+ in similar conditions is overlapped (Fig. 5B). This increased sensitivity in water is also indicating the importance of the surface charge density of the membrane on the transistor gating efficiency as well as the significant effect of the background electrolyte ion strength in the initial doping state of the channel. In distilled water, the gating effect into the channel is reduced because of the lack of cations that can electrify the membrane interface, thus producing a minimum effect on the conducting polymer. Under these conditions, the relative effect produced by the additions of K^+ are enhanced.

Calibration plots for K^+ in a 0.1 M NaCl and in a 0.1 M $MgCl_2$ were performed to evaluate the influence of high Na^+ background concentrations, as is common in clinical samples. Remarkably, there are not significant differences between them (Fig. 5C). Comparison of the analytical performance in different media can be seen in Fig. S6 and Table S3. Finally, basic characteristics of recently reported IS-OECTs are summarised in Table 2. Additionally, a paper-based ion-selective electrode was added for comparison. These results stress the outstanding performance of the IS-OECT presented in this work.

3.3. Determination of K^+ at clinical levels

The normal levels of K^+ in blood range from 3.6 to 5.2 mM. Slight differences beyond this range are life-threatening and require immediate medical attention. To evaluate the power of the IS-OECT in this scenario, a calibration curve in artificial serum for K^+ in the range 1–10 mM was performed (Fig. 5D) For a small portion of this curve -the interval 3–7 mM- the relationship was linearized, yielding a calibration plot with a sensitivity of 84.6 ± 4.4 μA/mM (Fig. 5E). These results show that the system has a good power of discriminating small variations in concentration, even at these relatively high levels of the analyte and in high levels of a background electrolyte. A time trace for an

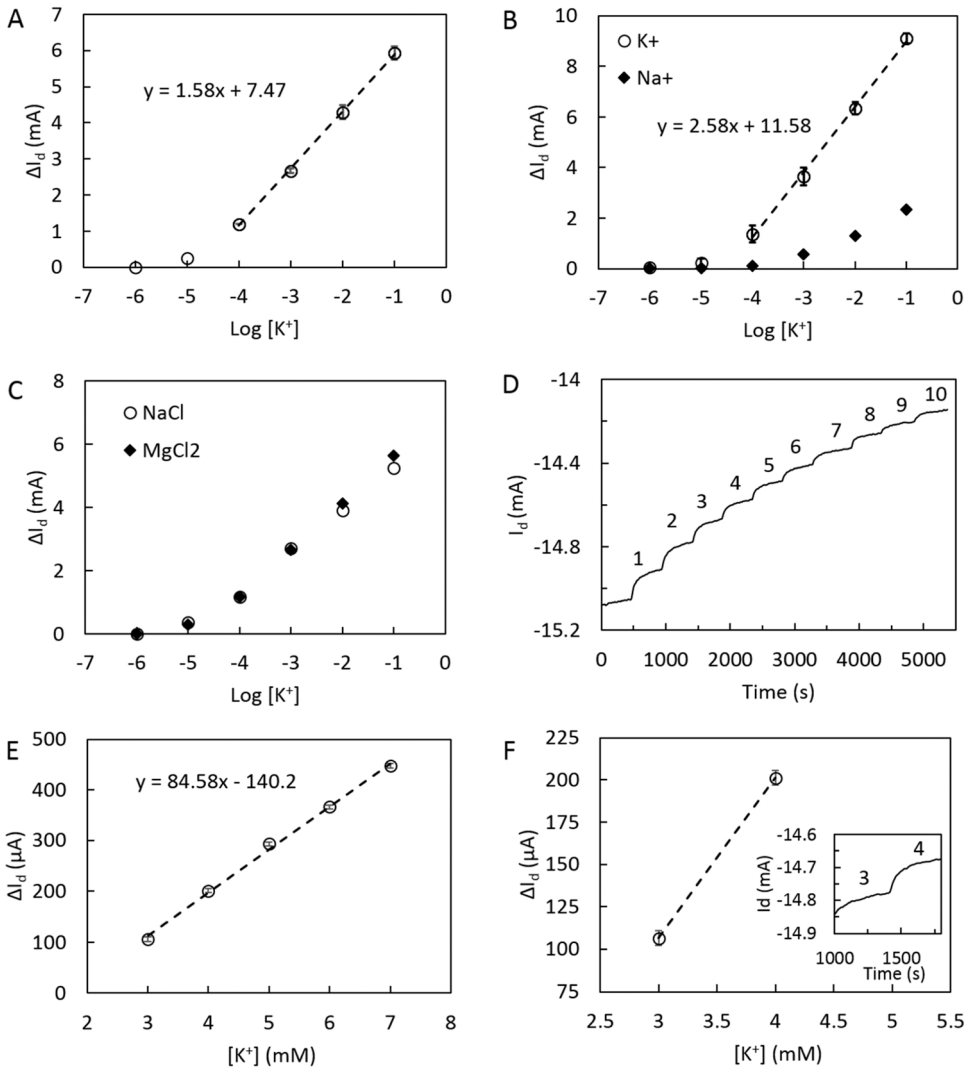

Fig. 5. : A) K^+ calibration curve corresponding to 4 different sensors in 0.1 $MgCl_2$. Error bars can be seen within the markers B) K^+ and Na^+ calibration curves in H_2O for 3 different sensors. C) Comparison of K^+ calibration curve in 0.1 M NaCl and $MgCl_2$ D) Time trace upon increasing additions of K^+, from 1 to 10 mM, in artificial serum. E) Corresponding calibration curve linearized in the 3–7 mM with a sensitivity of 84.58 ± 4.4 μA/mM. F) Inset of the calibration curve and time trace corresponding to the addition of 4 mM. In all the experiments V_g = –0.4 V and V_d = 0 V.

Table 2
Performance of recent K^+ IS-OECTs manufactured with different approaches and of a paper-based ion-selective electrode. Sensitivity are reported in μA/decade and/or mV/decade.

Device	Sensitivity (μA/decade)	Sensitivity (mV/decade)	Fabrication process	Substrate	Reference
Paper based ISE		58.1 ± 0.7	Ink painting and casting	Paper	[30]
Gel electrolyte based OECT	47	48	Photolithography	Glass substrate	[28]
Wearable flexible OECT	7.5 ± 1.5	–	Inkjet printing	Flexible polyimide foil	[35]
IS-OECT with PSS ion reservoir	224	84	Photolithography	Glass substrate	[29]
Complementary amplifier OECT		2344	Photolithography	Glass substrate	[37]
Single component IS-OECT	49	–	Photolithography	Flexible polyimide film	[38]
Paper-based IS OECT	2586 ± 58	–	Drop casting	Paper	This work

increment in concentration from 3 to 4 mM is shown in Fig. 5F. Recalling that the noise levels of the system are in the order of 0.8 μA, changes in concentration down to 0.05 mM could be easily discriminated. Therefore, without additional amplification of the signal the device presented here shows a very good performance for this type of application.

4. Conclusions

This work has presented an approach to build highly sensitive IS-OECT. It is shown that instead of the traditional thin-channel/thick membrane approach, a combination of a thick conducting polymer film with a careful optimization of the membrane composition and thickness allows achieving high sensitivity while preserving the selectivity. As a result, outstanding analytical performance can be achieved even at high saline concentration. While the linear range is only 3 orders

of magnitude -lower than the typically obtained for ion-selective electrodes-, the work has been mostly focused on the optimization for detection at high analyte concentrations. Further optimization could help to improve limits of detection and linear ranges. From a design perspective, this approach provides a path to build simple, robust, highly reproducible, and affordable paper-based sensors using a simple printing process that does not require microfabrication techniques.

The operation at and optimum $V_{gmax} = 0$ V provides ways to design more compact systems, avoiding the gate power supply. Alternatively, at high V_g the unspecific charging of the membrane may provide ways for the determination of the total ion activity. These features, controlled through the gate potential, may open interesting avenues for the determination of ions in the point of need.

CRediT authorship contribution statement

Conceptualization: FJA. Methodology: MCE, AAY, PB and FJA. Investigation: MCE, AAY, PB. Supervision: PB and FJA. Resources: FJA. Writing–original draft: FJA. Writing–review & editing: all co-authors.

Declaration of Competing Interest

The authors declare that they have no known competing financial interests or personal relationships that could have appeared to influence the work reported in this paper.

Data Availability

Data will be made available on request.

Acknowledgements

The authors would like to acknowledge the financial support from the Spanish ministry of Science and innovation and the state agency of research (AEI) (PID2019-106862RB-I00 / AEI / 10.13039/501100011033).

Appendix A. Supporting information

Supplementary data associated with this article can be found in the online version at doi:10.1016/j.snb.2023.135027.

References

[1] E. Zdrachek, E. Bakker, Potentiometric sensing, Anal. Chem. 91 (2019) 2–26, https://doi.org/10.1021/acs.analchem.8b04681.
[2] M. Cuartero, E. Bakker, Environmental water analysis with membrane electrodes, Curr. Opin. Electrochem. 3 (2017) 97–105, https://doi.org/10.1016/j.coelec.2017.06.010.
[3] R. Yan, S. Qiu, L. Tong, Y. Qian, Review of progresses on clinical applications of ion selective electrodes for electrolytic ion tests: from conventional ISEs to graphene-based ISEs, Chem. Speciat. Bioavailab. 28 (2016) 72–77, https://doi.org/10.1080/09542299.2016.1169560.
[4] M. Novell, N. Rico, P. Blondeau, M. Blasco, A. Maceira, J.L. Bedini, F.J. Andrade, F. Maduell, A novel point-of-care device for blood potassium detection of patients on dialysis: comparison with a reference method, Nefrología 40 (2020) 363–364, https://doi.org/10.1016/j.nefro.2019.06.002.
[5] Y. Shao, Y. Ying, J. Ping, Recent advances in solid-contact ion-selective electrodes: functional materials, transduction mechanisms, and development trends, Chem. Soc. Rev. 49 (2020) 4405–4465, https://doi.org/10.1039/C9CS00587K.
[6] C.-S. Lee, S.K. Kim, M. Kim, Ion-sensitive field-effect transistor for biological sensing, Sens. (Basel) 9 (2009) 7111–7131, https://doi.org/10.3390/s90907111.
[7] S. Yuvaraja, A. Nawaz, Q. Liu, D. Dubal, S.G. Surya, K.N. Salama, P. Sonar, Organic field-effect transistor-based flexible sensors, Chem. Soc. Rev. 49 (2020) 3423–3460, https://doi.org/10.1039/C9CS00811J.
[8] U. Vanamo, E. Hupa, V. Yrjänä, J. Bobacka, New signal readout principle for solid-contact ion-selective electrodes, Anal. Chem. 88 (2016) 4369–4374, https://doi.org/10.1021/acs.analchem.5b04800.
[9] P. Kraikaew, S. Jeanneret, Y. Soda, T. Cherubini, E. Bakker, Ultrasensitive seawater ph measurement by capacitive readout of potentiometric sensors, ACS Sens. 5 (2020) 650–654, https://doi.org/10.1021/acssensors.0c00031.
[10] E. Zdrachek, E. Bakker, Potentiometric sensor array with multi-nernstian slope, Anal. Chem. 92 (2020) 2926–2930, https://doi.org/10.1021/acs.analchem.9b05187.
[11] J. Rivnay, S. Inal, A. Salleo, R.M. Owens, M. Berggren, G.G. Malliaras, Organic electrochemical transistors, 2018 32, Nat. Rev. Mater. 3 (2018) 1–14, https://doi.org/10.1038/natrevmats.2017.86.
[12] E. Macchia, R.A. Picca, K. Manoli, C. Di Franco, D. Blasi, L. Sarcina, N. Ditaranto, N. Cioffi, R. Österbacka, G. Scamarcio, F. Torricelli, L. Torsi, About the amplification factors in organic bioelectronic sensors, Mater. Horiz. 7 (2020) 999–1013, https://doi.org/10.1039/C9MH01544B.
[13] H.S. White, G.P. Kittlesen, M.S. Wrighton, Chemical derivatization of an array of three gold microelectrodes with polypyrrole: fabrication of a molecule-based transistor, J. Am. Chem. Soc. 106 (1984) 5375–5377, https://doi.org/10.1021/ja00330a070.
[14] D.A. Bernards, G.G. Malliaras, Steady-state and transient behavior of organic electrochemical transistors, Adv. Funct. Mater. 17 (2007) 3538–3544, https://doi.org/10.1002/adfm.200601239.
[15] D. Nilsson, T. Kugler, P.O. Svensson, M. Berggren, An all-organic sensor-transistor based on a novel electrochemical transducer concept printed electrochemical sensors on paper, Sens. Actuators B Chem. 86 (2002) 193–197, https://doi.org/10.1016/S0925-4005(02)00170-3.
[16] F. Mariani, I. Gualandi, M. Tessarolo, B. Fraboni, E. Scavetta, PEDOt: dye-based, flexible organic electrochemical transistor for highly sensitive ph monitoring, ACS Appl. Mater. Interfaces 10 (2018) 22474–22484, https://doi.org/10.1021/acsami.8b04970.
[17] A. Ait Yazza, P. Blondeau, F.J. Andrade, Simple approach for building high transconductance paper-based organic electrochemical transistor (oect) for chemical sensing, ACS Appl. Electron. Mater. 3 (2021) 1886–1895, https://doi.org/10.1021/ACSAELM.1C00116.
[18] H. Tang, F. Yan, P. Lin, J. Xu, H.L.W. Chan, Highly sensitive glucose biosensors based on organic electrochemical transistors using platinum gate electrodes modified with enzyme and nanomaterials, Adv. Funct. Mater. 21 (2011) 2264–2272, https://doi.org/10.1002/adfm.201002117.
[19] E. Bihar, Y. Deng, T. Miyake, M. Saadaoui, G.G. Malliaras, M. Rolandi, A disposable paper breathalyzer with an alcohol sensing organic electrochemical transistor, Sci. Rep. 6 (2016) 2–7, https://doi.org/10.1038/srep27582.
[20] D.J. Kim, N.E. Lee, J.S. Park, I.J. Park, J.G. Kim, H.J. Cho, Organic electrochemical transistor based immunosensor for prostate specific antigen (PSA) detection using gold nanoparticles for signal amplification, Biosens. Bioelectron. 25 (2010) 2477–2482, https://doi.org/10.1016/j.bios.2010.04.013.
[21] J. Liao, H. Si, X. Zhang, S. Lin, Functional sensing interfaces of pedot:pss organic electrochemical transistors for chemical and biological sensors: a mini review, Sens. (Basel) 19 (2019) 218, https://doi.org/10.3390/s19020218.
[22] S.T. Keene, D. Fogarty, R. Cooke, C.D. Casadevall, A. Salleo, O. Parlak, Wearable organic electrochemical transistor patch for multiplexed sensing of calcium and ammonium ions from human perspiration, Adv. Healthc. Mater. 8 (2019), 1901321, https://doi.org/10.1002/ADHM.201901321.
[23] Y. Li, B. Cui, S. Zhang, B. Li, J. Li, S. Liu, Q. Zhao, Y. Li, B. Li, J. Li, Q. Zhao, B. Cui, S. Zhang, S. Liu, Ion-selective organic electrochemical transistors: recent progress and challenges, Small (2022), 2107413, https://doi.org/10.1002/SMLL.202107413.
[24] I. Gualandi, M. Tessarolo, F. Mariani, L. Possanzini, E. Scavetta, B. Fraboni, Textile chemical sensors based on conductive polymers for the analysis of sweat, Polym. (Basel) 13 (2021) 894, https://doi.org/10.3390/polym13060894.
[25] I. Gualandi, M. Tessarolo, F. Mariani, D. Tonelli, B. Fraboni, E. Scavetta, Organic electrochemical transistors as versatile analytical potentiometric sensors, Front. Bioeng. Biotechnol. 7 (2019), https://doi.org/10.3389/fbioe.2019.00354.
[26] Z. Mousavi, A. Ekholm, J. Bobacka, A. Ivaska, Ion-selective organic electrochemical junction transistors based on poly(3,4-ethylenedioxythiophene) doped with poly (styrene sulfonate), Electroanalysis 21 (2009) 472–479, https://doi.org/10.1002/elan.200804427.
[27] J. Aerathupalathu Janardhanan, Y.-L. Chen, C.-T. Liu, H.-S. Tseng, P.-I. Wu, J.-W. She, Y.-S. Hsiao, H. Yu, Sensitive detection of sweat cortisol using an organic electrochemical transistor featuring nanostructured poly(3,4-ethylenedioxythiophene) derivatives in the channel layer, Anal. Chem. 94 (2022) 7584–7593, https://doi.org/10.1021/acs.analchem.2c00497.
[28] M. Sessolo, J. Rivnay, E. Bandiello, G.G. Malliaras, H.J. Bolink, Ion-selective organic electrochemical transistors, Adv. Mater. 26 (2014) 4803–4807, https://doi.org/10.1002/adma.201400731.
[29] S. Han, S. Yamamoto, A.G. Polyravas, G.G. Malliaras, Microfabricated ion-selective transistors with fast and super-nernstian response, Adv. Mater. 32 (2020) 1–8, https://doi.org/10.1002/adma.202004790.
[30] M. Novell, M. Parrilla, G.A. Crespo, F.X. Rius, F.J. Andrade, Paper-based ion-selective potentiometric sensors, Anal. Chem. 84 (2012) 4695–4702, https://doi.org/10.1021/ac202979j.
[31] E. Zeglio, O. Inganäs, Active materials for organic electrochemical transistors, Adv. Mater. 30 (2018), 1800941, https://doi.org/10.1002/ADMA.201800941.
[32] D. Khodagholy, J. Rivnay, M. Sessolo, M. Gurfinkel, P. Leleux, L.H. Jimison, E. Stavrinidou, T. Herve, S. Sanaur, R.M. Owens, G.G. Malliaras, High transconductance organic electrochemical transistors, 2013 41, Nat. Commun. 4 (2013) 1–6, https://doi.org/10.1038/ncomms3133.
[33] G.D. Spyropoulos, J.N. Gelinas, D. Khodagholy, Internal ion-gated organic electrochemical transistor: a building block for integrated bioelectronics, Sci. Adv. 5 (2019), eaau7378, https://doi.org/10.1126/sciadv.aau7378.

[34] K. Schmoltner, J. Kofler, A. Klug, E.J.W. List-Kratochvil, Electrolyte-gated organic field-effect transistor for selective reversible ion detection, Adv. Mater. 25 (2013) 6895–6899, https://doi.org/10.1002/adma.201303281.
[35] S. Demuru, B.P. Kunnel, D. Briand, Real-time multi-ion detection in the sweat concentration range enabled by flexible, printed, and microfluidics-integrated organic transistor arrays, Adv. Mater. Technol. 5 (2020), 2000328, https://doi.org/10.1002/ADMT.202000328.
[36] M. Braendlein, T. Lonjaret, P. Leleux, J.-M. Badier, G.G. Malliaras, Voltage amplifier based on organic electrochemical transistor, Adv. Sci. 4 (2017), 1600247, https://doi.org/10.1002/advs.201600247.
[37] P. Romele, P. Gkoupidenis, D.A. Koutsouras, K. Lieberth, Z.M. Kovács-Vajna, P.W. M. Blom, F. Torricelli, Multiscale real time and high sensitivity ion detection with complementary organic electrochemical transistors amplifier, Nat. Commun. 11 (2020) 1–11, https://doi.org/10.1038/s41467-020-17547-0.
[38] S. Wustoni, C. Combe, D. Ohayon, M.H. Akhtar, I. McCulloch, S. Inal, Membrane-free detection of metal cations with an organic electrochemical transistor, Adv. Funct. Mater. 29 (2019), 1904403, https://doi.org/10.1002/adfm.201904403.

Marc Clua Estivill received his Bsc in chemistry and master in nanoscience, materials and processes from the University Rovira i Vrigili (URV, Tarragona) in 2021. He then joined the research group of Nanosensors as a PhD student and he is currently developing new approaches to build electrochemical sensors for healthcare monitoring.

Adil Aït Yazza received his master in material science (University of Troyes, Franc, 2007), master in innovation and quality management (University of Metz, 20013) and master in nanoscience, materials and processes (University Rovira i Vrigili, Tarragona, 2019). He completed his PhD in the research group of Nanosensors in january 2023. His interests are the development of new hybrid materials for electrochemical sensing.

Pascal Blondeau received his PhD in chemistry (2007) at the University of Madrid (UAM) and then moved the University of Padova (Italy) for a post-doc position. He joined the Nanosensors research group at the University Rovira i Vrigili (URV, Tarragona) in 2009 where he is currently working as senior researcher. His research interests include the development of chemical sensors and platform for the sensing of biologically relevant markers. He is the co-founder of the company CreatSens Health and EOXSense.

Francisco J. Andrade received his PhD at the University of Buenos Aires (2002). He then worked as postdoctoral fellow and later as a faculty member in the Laboratory for Spectroscopy at Indiana University (USA). In 2007, he worked as Disruptive Team leader at Unilever Corporation (Leeds, UK) and then as Open Innovation Director. In 2010, he was awarded a Ramón y Cajal fellow at the research group of Nanosensors in the University Rovira I Virgili (Tarragona) where he is now professor of analytical chemistry and leader of the research group. His interest include the development of new analytical tools for the generation of biochemical information in the digital era. He is the co-founder of several technology-based companies from the same University (Kamelon Venture, CreatSens Health, EOXSense).